Published in : International Journal of Pharmaceutics (2018), vol. 549, pp. 161–168
DOI: 10.1016/j.ijpharm.2018.07.060
Status : Postprint (Author's version)

SULINDAC ENCAPSULATION AND RELEASE FROM FUNCTIONAL POLY(HEMA) MICROPARTICLES PREPARED IN SUPERCRITICAL CARBON DIOXIDE

Rahmet Parilti

CERM, CESAM Research Unit, University of Liege, 13, Allee du Six Août, B-4000 Liege, Belgium – School of Chemistry, University of Nottingham, University Park, NG7 2RD Nottingham, United Kingdom.

Raphaël Riva

CERM, CESAM Research Unit, University of Liege, 13, Allee du Six Août, B-4000 Liege, Belgium.

Steven M. Howdle

School of Chemistry, University of Nottingham, University Park, NG7 2RD Nottingham, United Kingdom.

Christine Dupont-Gillain

Institute of Condensed Matter and Nanosciences (IMCN), Bio and Soft Matter Division (BSMA), Université Catholique de Louvain, Place Louis Pasteur 1, 1348 Louvainla-Neuve, Belgium.

Christine Jerome*

CERM, CESAM Research Unit, University of Liege, 13, Allee du Six Août, B-4000 Liege, Belgium.

Abstract

Sulindac loaded poly(HEMA) cross-linked microparticles were synthesized via one-pot free-radical dispersion polymerisation in supercritical carbon dioxide (scCO2) in presence of photocleavable diblock stabilisers based on polyethylene oxide (PEO) and poly(heptadecafluorodecyl acrylate) (PFDA) bearing a o-nitrobenzyl photosensitive junction (hv) (PEO-hv-PFDA), and ethylene glycol dimethacrylate (EGDMA) as cross-linker. Poly(HEMA) cross-linked microparticles either empty or sulindac loaded were obtained with well-defined spherical morphology with the sizes between 250 and 350 nm. Additionally, upon UV-photolysis the stabiliser on the surface was cleaved which permits to microparticles to be redispersed in water leading to water swollen microgels about 2.1–3.6 µm. Moreover, the release behaviour from obtained microgels indicated the sustained release of sulindac over 10 days. Besides, the surface modification after UV-photolysis was studied and proved that the particles can be functionalised with further chemistries.

Published in : International Journal of Pharmaceutics (2018), vol. 549, pp. 161–168
DOI: 10.1016/j.ijpharm.2018.07.060
Status : Postprint (Author's version)

Keywords: 2-Hydroxyethyl methacrylate, Cross-linked particle, Microgel, Sulindac, Supercritical carbon dioxide.

1. Introduction

There has been a tremendous growth in the field of designing controlled delivery systems based on polymer carriers, one of them being hydrogel formulations based on (sub)microparticles referred also as micro- or nanogels. These systems combine the characteristics of both hydrogels and particles being a 3D network able to swell in water/ biological fluids and at the same time having a small size and large surface area (Hamidi et al., 2008). Unique features of these networks made them promising candidates to be used in biomedical fields such as tissue engineering, regenerative medicine, diagnostics and many more (Ryu et al., 2010).

These hydrogel particles can be easily prepared using heterogeneous free radical polymerisation techniques such as dispersion, inverse mini or micro emulsion by introducing a suitable difunctional monomer as cross-linker to the reaction mixture (Chacko et al., 2012). In dispersion polymerisation by using a proper stabiliser the formed polymers can be dispersed in the continuous phase resulting into spherical particles with sizes ranging between 100 nm and 10 µm with narrow size-distribution (Cao et al., 2006). In recent years, an increasing interest was devoted to the use of supercritical carbon dioxide, i.e. a non-toxic and environmental friendly solvent as medium for heterogeneous processes to produce particles (Jennings et al., 2013). Supercritical carbon dioxide ($scCO_2$) is a non-toxic, non-flammable, inexpensive and environmentally benign solvent with easily achievable critical point, i.e. T_c = 31.1 °C and P_c = 73.8 bar. The aforementioned moderate critical points of CO_2 allow processing conditions compatible with thermosensitive drugs. It is also an inert medium which prevents oxidation (Cocero et al., 2009). Moreover, upon depressurisation, CO_2 goes to gaseous state which offers dry condition at low temperature enabling to handle water, solvent and heat labile substances (Davies et al., 2008). Moreover, since the CO_2 can be removed from the media easily, energy consuming solvent removal stage is avoided which allows us to produce dry powder formulations (Miyazaki et al., 2017). Therefore, $scCO_2$ has taken great attention in pharmaceutical applications as a solvent or anti-solvent to either extract or process bioactive agents, most importantly a medium for producing drug loaded polymer particles with enhanced bioavailability (Nuchuchua et al., 2017).

Non-steroidal anti-inflammatory drugs (NSAID)s are frequently used for the treatment of acute and chronic inflammation and related pain. Therefore, they are prescribed in large quantities worldwide for the patients and their use is expected to rise in the future (Gerstein et al., 2014). For instance, aspirin, ibuprofen, diclofenac are some of the well-known and mostly used examples of NSAIDs. NSAIDs can be classified into different groups with respect to their chemical structure and sulindac falls into the indoleacetic acid group along with indometacin, tolmetin and ketorolac. We are specifically interested in sulindac since it was reported to have promising anti-proliferative activity towards different cancer types both in vitro and in vivo. For instance, sulindac was tested in cell lines of acute myeloid leukemia (AML) and primary cells from bone marrow of the patients (Singh et al., 2011).

Published in : International Journal of Pharmaceutics (2018), vol. 549, pp. 161–168
DOI: 10.1016/j.ijpharm.2018.07.060
Status : Postprint (Author's version)

Moreover, it is also found to relieve the pain from arthritis such as osteoarthritis and rheumatoid (Lee et al., 2010).

Even though in general NSAIDs are taken orally, they are either practically insoluble or sparingly soluble in aqueous environment; they have low bioavailability and show poor stability which results in storage problems. Also in long-term, they cause gastrointestinal side effects. Therefore to overcome these problems, studies are focused on encapsulation of the NSAIDs into polymeric carriers (Badri et al., 2016). Ammar et al. have prepared chitosan and carboxymethyl-β-cyclodextrin (CM-β-CD) cross-linked nanoparticles for the encapsulation of sulindac (Ammar et al., 2012). Carmona-Moran et al. have encapsulated diclofenac (NSAID) in poly(N-vinylcaprolactam)-co-acrylic acid core-shell nanogels and embedded in the solid hydrogel matrix for transdermal applications (Carmona-Moran et al., 2016). Choudhary et al. encapsulated sulindac in hydrophobically modified alginate gels. However, in the preparation of these nanogels, extensive purification time (i.e. 4 weeks) is required before loading the drug by impregnation or diffusion (Choudhary et al., 2017). In addition to these hydrogels, poly (2-hydroxyethyl methacrylate) (poly(HEMA)) was also investigated previously by Andrade-Vivero et al. to be used for the delivery of diclofenac and ibuprofen (NSAID)s (Andrade-vivero et al., 2007).

2-hydroxyethyl methacrylate is a hydrophilic monomer and its homo- or copolymers find well-established biomedical applications (Abraham et al., 2005; Cadotte and Demarse, 2005; González-Chomón et al., 2012). The poly(HEMA) hydrogels are widely used to deliver drugs from drug-eluting implants (Long et al., 2014; Macková et al., 2017) in reconstructive materials in dental applications (Kitagawa et al., 2014), in ocular treatment (Garcia-Millan et al., 2015) and also to deliver proteins (Hackl et al., 2017).

The aim of the present paper is to produce well-defined and submicronic poly(HEMA) particles encapsulating sulindac by dispersion polymerisation in supercritical carbon dioxide. As already reported by Ma and Lacroix-desmazes (2004) polyethylene oxide (PEO) block poly (heptadecafluorodecyl acrylate) (PFDA) (PEO-*b*-PFDA) diblock copolymers are efficient stabilisers for the poly(HEMA) particles in supercritical carbon dioxide. In addition, some of us have also reported mild conditions, especially low temperature (35 °C) for HEMA dispersion polymerisation in $scCO_2$ giving well-defined and small sized particles (216 nm) (Parilti et al., 2017) (Scheme 1, step 1). In addition, Alaimo et al. have shown that the use of a photocleavable junction between the polyethylene oxide (PEO) and poly(heptadecafluorodecyl acrylate) (PFDA) blocks of the stabiliser (PEO-h*v*-PFDA) allows to remove the fluorinated block after the particles synthesis and as a consequence allows the poly(HEMA) particles to swell in water (Scheme 1, step 2) (Alaimo et al., 2017).

Published in : International Journal of Pharmaceutics (2018), vol. 549, pp. 161–168
DOI: 10.1016/j.ijpharm.2018.07.060
Status : Postprint (Author's version)

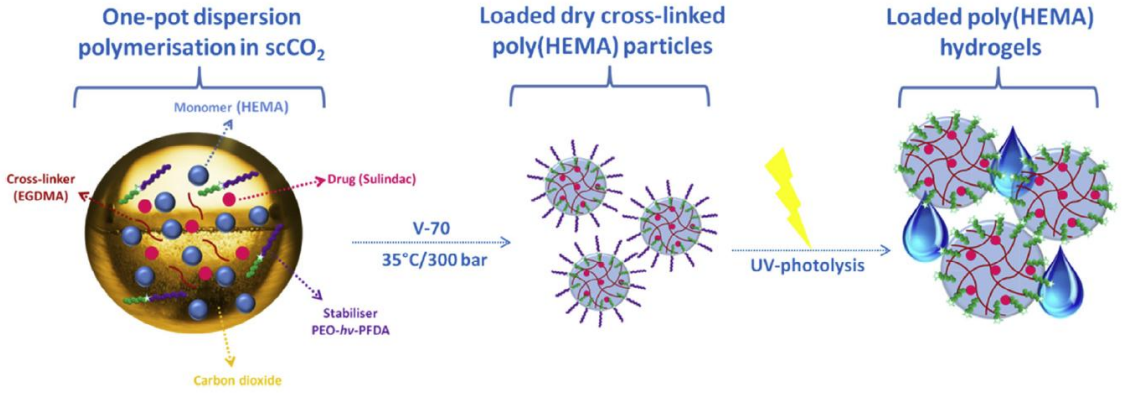

Scheme 1. Synthetic approach to obtain sulindac loaded poly(HEMA) hydrogels in supercritical carbon dioxide($scCO_2$) using photocleavable stabilisers.

In the present paper, we have studied further such process targeting the one-pot encapsulation of sulindac, by adding the drug from the beginning of the process. Therefore, the effect of the presence of the drug on the particle size and overall particles properties has been evaluated. The drug encapsulation and release profile in aqueous media are also reported here.

2. Experimental part

2.1. MATERIALS

All chemicals are purchased from Sigma-Aldrich and used as received unless otherwise it is noted. Sulindac (≥98.0%), fluoresceinamine, isomer I, sodium cyanoborohydride (1.0 M in THF), 2,2'Azobis(4-methoxy-2,4-dimethylvaleronitrile) (V-70,Wako), 2-hydroxyethyl methacrylate (HEMA, Aldrich, 97%), ethylene glycol dimethacrylate (EGDMA, Aldrich, 98%), carbon dioxide (I5122,CO2 N27 purity > 99,999%, Air Liquide, Belgium). α,α,α-Trifluorotoluene (TFT, Aldrich, 99+%). Ultrapure water was produced by MilliQ plus 188 apparatus (Millipore). SpectraPor membrane (cut-off 3.5 kDa and 1 kDa). PEO_{45}-h*v*-$PFDA_{50}$ diblock copolymer bearing a photocleavable junction was synthesized according to previously published procedure (Alaimo et al., 2017).

2.2. METHODS

2.2.1. SYNTHESIS OF THE SULINDAC ENCAPSULATED POLY(HEMA) NETWORKS IN $SCCO_2$

Dispersion polymerisations of 2-hydroxyethyl methacrylate were performed as previously described by Parilti et al. (2017). The procedure can be described as follows: the high pressure stainless steel cell (82 ml, ToP Industrie) was charged with 8.2 ml of HEMA (10% v/v CO_2), 400 µl of EGDMA (cross-linker, 5% v/v monomer), 0.82 g of stabiliser, 0.187 g V-70 (1% w/v monomer) and 8.79 mg/87.9 mg sulindac (0.1% or 1% with respect to w_{HEMA}). The cell was securely sealed and a small amount of CO_2 was introduced using a syringe pump (ISCO model no. 260D). After the heating mantel was clamped, the stirring rate (400 rpm) and temperature (35 °C) were set with the control unit.

Published in : International Journal of Pharmaceutics (2018), vol. 549, pp. 161–168
DOI: 10.1016/j.ijpharm.2018.07.060
Status : Postprint (Author's version)

Temperature and pressure were increased step-wise, the reactor was stabilised at the desired conditions (35 °C/300 bar) and the reaction was left for stirring overnight. At the end of the reaction, stirring was stopped and the heating jacket removed allowing the reactor to cool down to ambient temperature. Thereafter, the reactor is depressurized gradually by opening an outlet valve. After total depressurization, the cell was opened and the product was collected as a dry powder. Obtained products were stored in the ambient temperature in a plastic container.

2.2.2. UV PHOTOLYSIS OF THE PARTICLES

The particles were dispersed in TFT with the concentration of 10 mg/ml. The solution was sonicated using horn sonicator for about 3 min resulting into a milky dispersion. Thereafter solution was subjected to UV under vigorous stirring (700 rpm) using UV lamp (LOTOriel Arc Light Source Hg(Xe), power = 500 W, with multichromatic emission showing the characteristic emission at 300–310 nm for the photocleavage of o-nitrobenzyl groups. The UV exposure times were varied from 30 min to 60 min.

2.2.3. RELEASE BEHAVIOR

After fluorine extraction, 50 mg of particles were placed into a dialysis membrane with a cut off of 100 kDa (SpectraPor® membrane) and 5 ml of Milli-Q water was then added (concentration 10 mg/ml). The membrane was placed in brown glass bottle with 100 ml of Milli-Q water (in sink conditions) and left for shaking in an orbital stirrer at 37 °C at a speed of 50 rpm. Samples (1 ml) were taken from the external medium of the membrane in different time intervals, and 1 ml of fresh Milli-Q water was added to keep the volume constant. The withdrawals were measured with UV–vis spectrometer (Shimadzu UV-1800). In order to calculate the amount of released sulindac, the absorbance was taken at 286 nm then converted to mass (µg) using a calibration curve. All the release experiments were performed in triplicate.

2.2.4. GRAFTING OF FLUORESCEINAMINE ON THE PARTICLES VIA REDUCTIVE AMINATION

Grafting of the fluoresceinamine was performed according to previously published conditions (Freichels et al., 2012). The procedure is described as follows: the UV-cleaved particles (100 mg, 1 equivalent of aldehyde groups) were suspended in 50 ml of phosphate buffer solution (500 mM, pH: 7.4) and fluoresceinamine isomer 1 (2 equivalents) was added. After 1 h of stirring, a 10-fold excess sodium cyanaborohydride solution (1.0 M in THF) was added. The mixture was left for stirring for 96 h and then dialyzed against water for 3 days by changing water for 4 times per day. Particles were recovered by rotary evaporator and freeze-drying.

2.3. CHARACTERISATION

All the particles were analyzed with scanning electron microscopy (SEM, JEOL JSM 840-A) to evaluate their morphology. Samples were prepared on SEM stubs and coated with Pt (30 nm). Particles average sizes were calculated from SEM images by random sampling of 75–100 particles with the aid of VistaMetrix software (version 1.33.0). Coefficient of variance (C_v) is an indicator of size distribution of the particles. It is calculated from the standard deviation (σ) divided by the average diameter size

Published in : International Journal of Pharmaceutics (2018), vol. 549, pp. 161–168
DOI: 10.1016/j.ijpharm.2018.07.060
Status : Postprint (Author's version)

(D_n) that is calculated from the SEM images (C_v =(σ/D_n)* 100) (Eq. (1)). Transmission electron microscopy (TEM, PHILIPS M100) operating at an accelerating voltage of 100 kV was used to further evaluate the particles size. TEM samples were prepared by placing a drop of diluted dispersion of particles on a TEM grid and left for air drying. The size distribution of particles in suspension in diluted TFT (before UV) and in water (after UV) were estimated by dynamic light scattering (DLS) using a Delsa Nano C Beckman Coulter at 25 °C. The DLS measurements were performed in triplicate for each sample. The intensity of scattered light was detected at 165° to the incident beam and data treated by the cumulant analysis. X-ray photoelectron Spectroscopy (XPS) analyses were performed on a SSX 100/206 spectrometer (Surface Science Instruments – USA) equipped with a monochromatized micro-focused aluminum X-ray source (powered at 20 mA and 10 kV). A flood gun set at 6eV and a Ni grid placed 3 mm above the sample surface were used for charge stabilisation. The angle between the surface normal and the axis of the analyser lens was 55°; in these conditions, the probed depth was of the order of 5 nm. The molar fractions were calculated from the peak areas normalized on the basis of the acquisition parameters and sensitivity factors provided by the manufacturer. The calculations exclude hydrogen which is not detected by XPS. Carbon and fluorine spectra recorded second time after the analysis in order to validate that the sample was not degraded by X-ray source. The data analysis was performed with the CasaXPS program (Casa Softwares, Teignmouth, UK).

3. Results and discussion

3.1. ONE-POT SULINDAC ENCAPSULATION BY IN-SITU DISPERSION POLYMERISATION OF HEMA

The one-pot encapsulation of sulindac into cross-linked poly(HEMA) particles has been first studied by following a previously reported supercritical CO_2 process. Indeed, mild reaction conditions (35 °C and 300 bar) were reported previously (Parilti et al., 2017) to synthesize well-defined poly(HEMA) particles by dispersion polymerisation in $scCO_2$. Following such process, the monomer, HEMA (10% v/v CO_2), the cross-linker, EGDMA (5% v/v monomer), the photocleavable stabiliser, PEO_{45}-h*v*-$PFDA_{50}$ (0.82 g) and the initiator, V-70 (1% w/v monomer) were introduced in the high-pressure cell, together with the sulindac in order to perform its one-pot encapsulation. Two different concentrations of sulindac 0.1% and 1% with respect to monomer (%,$w_{sulindac}/w_{HEMA}$) have been tested. After polymerization at 35 °C under 300 bar for at least 18 h, the reactor is depressurized and a dry powder is collected. Let us mention that thanks to the solubility of the HEMA monomer and residual initiator in $scCO_2$, potential traces of unreacted HEMA after reaction would be extracted during venting. However, this was not extensively observed since full conversion is expected. Therefore, the collected powder can be used as collected from the reactor without requiring further purification process. The collected powder is first analysed by scanning and transmission electron microscopy (SEM/TEM). The overall characteristics of the obtained particles in presence of sulindac are reported in Table 1 and the

Published in : International Journal of Pharmaceutics (2018), vol. 549, pp. 161–168
DOI: 10.1016/j.ijpharm.2018.07.060
Status : Postprint (Author's version)

corresponding SEM and TEM images are reported in Fig. 1. They are compared to particles prepared in the same conditions but in absence of sulindac (Table 1, Entry 1; Figs. 1, 1a and 1b).

As evidenced by the SEM image of Fig. 1.1, the empty cross-linked poly(HEMA) particles exhibit a highly uniform spherical shape of small sizes, 348 nm. This was confirmed by TEM image (Fig. 1-1a and 1b) giving a size of 230 nm. For TEM measurement, the particles were suspended in tetrahydrofuran (THF) and a drop was placed on the TEM grid whereas for SEM, TFT, a good solvent for the stabiliser on the surface, was used. Therefore, difference between SEM size (348 nm) and TEM (2 3 0) results from different swelling state during sample preparation. As shown on Fig. 1.2 and 1.3, the addition of sulindac to the reaction medium does not affect the particles formation, shape and dispersity. Table 1 also shows that the particles size, measured by SEM or DLS, is not significantly modified by the presence of 1% of sulindac. Only the particles prepared in presence of 0.1% sulindac are slightly bigger.

Table 1
Characteristics of the powder as collected after $scCO_2$ dispersion polymerisation.

Entry	Initial sulindac[a] ($\%, w_{sulindac}/w_{HEMA}$)	SEM (nm)	C_v	DLS (nm)	Free sulindac[c] (%)
1	0	348	8	256[b]	–
2	0.1	561	6	328[b]	18.3
3	1	336	9	280[b]	1.8

a: Amount of sulindac added in the reactor before polymerization.
b: Measurement taken in trifluorotoluene (TFT).
c: Amount of free sulindac in the collected dry powder ($w_{free\ sulindac}/w_{initial\ sulindac}$ 100).

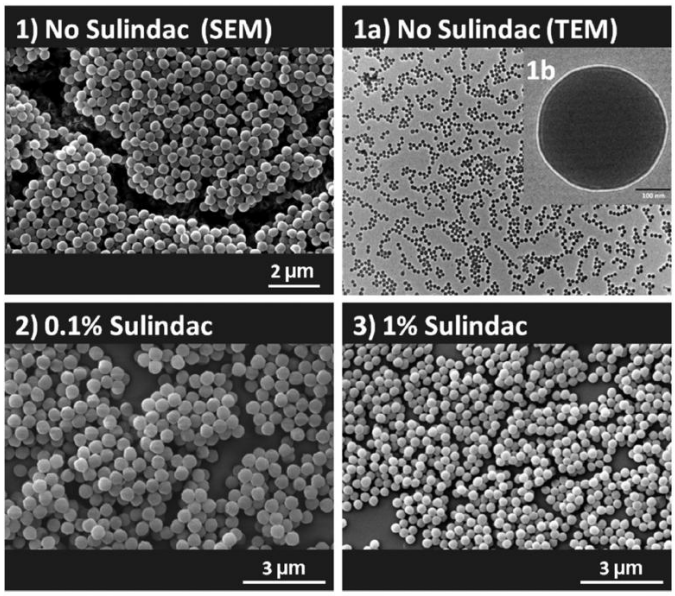

Fig. 1. SEM image of the poly(HEMA) particles 1) without sulindac, 2) with 0.1% sulindac and 3) with 1% sulindac; and (1a and 1b) TEM image without sulindac (1b scale bar 100 nm).

Published in : International Journal of Pharmaceutics (2018), vol. 549, pp. 161–168
DOI: 10.1016/j.ijpharm.2018.07.060
Status : Postprint (Author's version)

The dry particles collected after depressurization of the reactor are expected to be composed of a poly(HEMA) network loaded by the sulindac and coated at their surface by the fluorinated stabiliser which prevents their dispersion and swelling in water as illustrated in Fig. 2.1. In order to evaluate the amount of free sulindac that is not encapsulated in the particles, the dry powder collected from the high-pressure reactor was suspended in water under vigorous stirring (app. 750 rpm for 1 h) to insure their contact with water despite the fluorinated corona. By this way, only the sulindac which is adsorbed at the particles surface or that remains non-encapsulated in the particles would be able to dissolve in water. After filtration on 0.2 µm filter in order to remove the particles, the UV–vis absorptions (286 nm) of the aqueous solutions were recorded and converted to mass of sulindac using a previously recorded calibration curve (Guerra et al., 2016). Based on these UV–VIS data, the amount of free sulindac were found to be 18.3% for 0.1 wt% sulindac (Table 1-Entry 2) and 1.8% for 1 wt% starting sulindac content (Table 1-Entry 3). This shows that especially in the case of 1 wt% sulindac, very few amount of sulindac remains free at the term of the $scCO_2$ process due to the high solubility of sulindac in HEMA and poor solubility in $scCO_2$.

As shown in Fig. 2.1, the dry particles collected after depressurization of the reactor are cannot be dispersed directly in water due to the hydrophobic external corona formed by the fluorinated block (PFDA) of the stabiliser. Before release experiments, the fluorinated block of the stabiliser was thus removed thanks to the photocleavable link placed at the junction of both blocks.

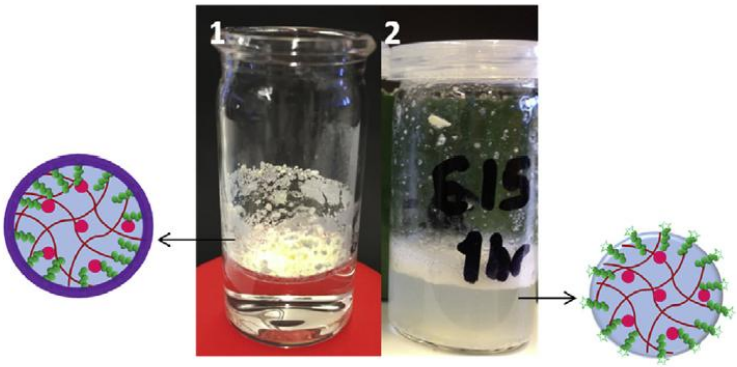

Fig. 2. Sulindac loaded poly(HEMA) networks dispersed in water before UV (1), dispersed in water after UV (2).

For this end, sulindac encapsulated particles were subjected to UVphotolysis (Scheme 2) in TFT, i.e. a good solvent for the fluorinated block which does not swell the poly(HEMA) network. After 30 min or 60 min, the irradiation was stopped and the samples were washed with fresh TFT to remove the cleaved fluorinated block and dried under vacuum. Since polyHEMA does not swell at all in TFT and since sulindac is insoluble in TFT, the release of sulindac cannot start during this step. Only the sulindac that would be trapped in the fluorinated shell could be lost. In addition, the solid poly(HEMA) network surrounding the sulindac might preserve it from UV photodegradation. As it is evidenced from the SEM images (Fig. 3) despite the aggregation of the particles, their shape was preserved after UV and extraction of the fluorinated block (Scheme 2 – step 1).

Published in : International Journal of Pharmaceutics (2018), vol. 549, pp. 161–168
DOI: 10.1016/j.ijpharm.2018.07.060
Status : Postprint (Author's version)

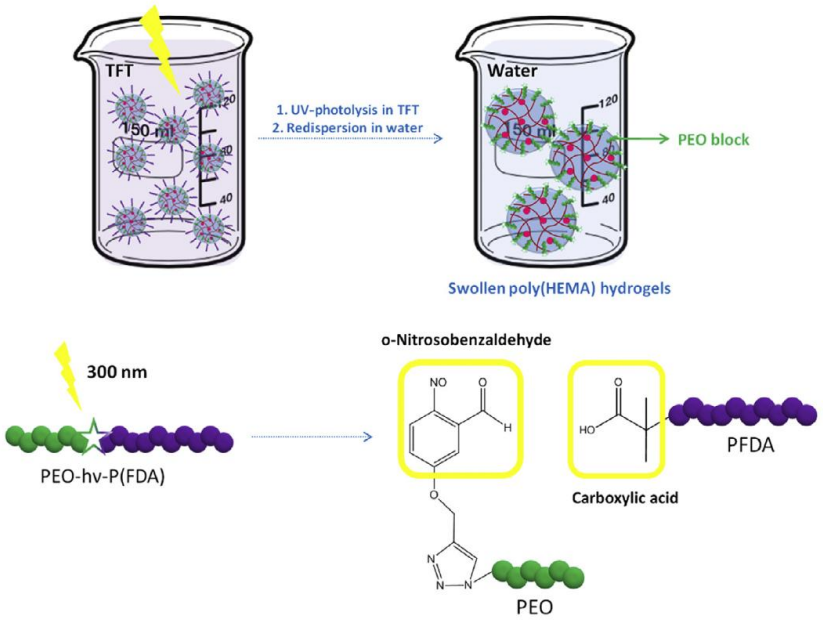

Scheme 2. UV-photolysis of the obtained poly (HEMA) particles were performed in TFT. Photocleavage of the stabiliser leads to formation of the o-nitrosobenzaldehyde groups on the particle surface and subsequently fluorinated block is extracted. The photo-isomerisation of the stabiliser results in the cleavage of the PEO-*hv*-PFDA stabiliser into first block (PEO) bearing nitrosobenzaldehyde group and carboxylic acid group at the end of second block (PFDA).

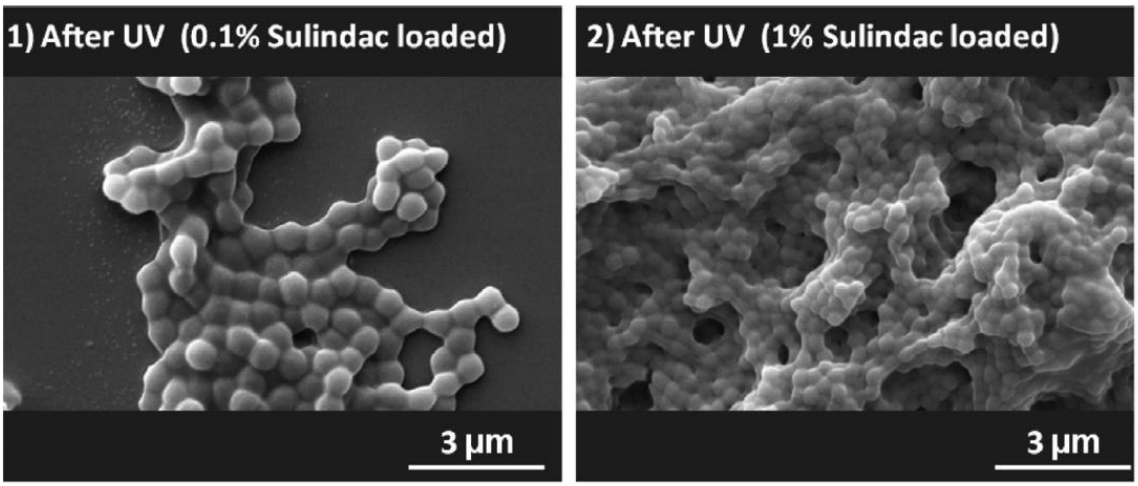

Fig. 3. SEM images of the sulindac (0.1% and 1% loaded poly(HEMA) particles after 1 h UV-photolysis (scale bar 3 µm).

For each sample, the efficiency of removal of the fluorinated layer from the particles was determined by X-ray photoelectron spectroscopy (XPS) by comparing the evolution of the total F/C ratios of the particles before and after photolysis of different durations (Table 2).

Published in : International Journal of Pharmaceutics (2018), vol. 549, pp. 161–168
DOI: 10.1016/j.ijpharm.2018.07.060
Status : Postprint (Author's version)

Table 2
XPS and DLS analyses of sulindac loaded poly(HEMA) particles for various times of UV-irradiation.

Entry	Sulindac (%,$w_{sulindac}$/w_{HEMA})	UV-Time (mins)	F/C (tot) (XPS)	Fluorine Extraction (%)	Particle Size (DLS)[a,b]
1	0.1	0	0.89	–	328 nm[a]
2	1	0	0.73	–	280 nm[a]
3	0.1	30	0.52	41.5	2.1 μm[b]
4	0.1	60	0.47	47.1	2.6 μm[b]
5	1	30	0.44	36.7	2.7 μm[b]
6	1	60	0.35	52.0	3.6 μm[b]

a: in trifluorotoluene (TFT) b: in water.

Table 2 clearly evidences that the fluorine content of the particles decreases for increasing UV-irradiation times. In previous work, Alaimo et al.[28] reported on the kinetics of particles photolysis using 0.1 mg particle/ml of TFT (LOT-Oriel UV-lamp was used) and fluorine extraction in TFT. According to the reported results, after 30 min of irradiation 72% of fluorine could be extracted. The kinetics of photocleavage reached to a plateau after 30 min and maximum extraction was reached after 6 h (79% fluorine extraction).

In our case, the photocleavage time was set to relatively short times (30 min and 60 min) in order to prevent degradation of the guest molecule. Moreover, the concentration of the particle dispersion for photocleavage was increased to 10 mg/ml, to lower the TFT amount. Therefore, direct comparison between these studies cannot be drawn but they are roughly giving similar fluorine extraction efficiency.

In this case, one hour of irradiation leads to the removal of half of the PFDA block from the particles surface. After this treatment, the resulting particles become dispersable in water (Fig. 2-2) and are able to swell thanks to the strong hydrophilicity of poly(HEMA) (Scheme 2 – step 2). This water swelling was clearly evidenced by DLS. In water, there is a significant increase of the particle size of at least one order of magnitude in each case. This shows that even if some fluorinated chains remain at the particles surface, the cross-linked poly(HEMA) are remarkably able to swell in water (36% of extracted fluorine leads already to a size increase from 271 nm to 2.7 μm). This shows the relatively low impact of the remaining fluorine chains on the particles swelling in water more importantly it does not prevent their water dispersion.

3.2. DETERMINATION OF THE PARTICLES LOADING AND RELEASE BEHAVIOUR.

Firstly, the barrier effect of the fluorinated corona of the particles towards the diffusion of sulindac to water was investigated. The particles (15 mg) loaded with 1% sulindac (Table 2-Entries 2, 5 and 6) before photolysis, after 30 min or 1 h exposure to UV light, have been dispersed in water and stirred for 24 h. The amount of released sulindac was then determined by UV–vis measurements. Fig. 4 clearly shows that the particles before UV treatment limit the release of sulindac to 2.4 μg, i.e. 1.5%.

Published in : International Journal of Pharmaceutics (2018), vol. 549, pp. 161–168
DOI: 10.1016/j.ijpharm.2018.07.060
Status : Postprint (Author's version)

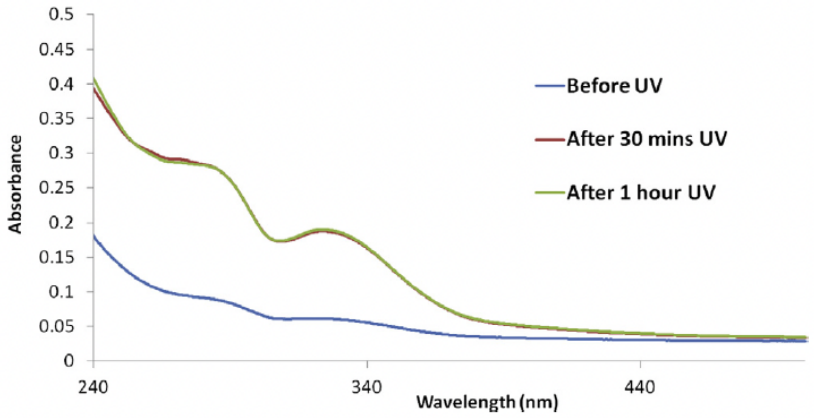

Fig. 4. UV–Vis spectra of released sulindac in water from 1% sulindac loaded particles (Table 2-Entry 2) Blue: without UV treatment (Table 2-Entry 2); Red: after 30 min of UV treatment (Table 2-Entry 5); Green after 1 h of UV treatment (Table 2-Entry 6).

After photolysis and partial removal of the fluorinated corona, the amount of released sulindac increased to approximately 10 µg for both particles subjected to different UV-irradiation times (30 min and 1 h). This clearly shows that the fluorinated corona acts as a barrier towards the sulindac diffusion however this barrier effect is clearly decreased already after short time of UV irradiation (30 min).

Then, the release profile in water and in sink conditions of the hydrogel particles synthesized by loading the $scCO_2$ reactor with 1% sulindac and exposed to 1 h UV for removal of the fluorinated block was monitored during 37 days (Fig. 5).

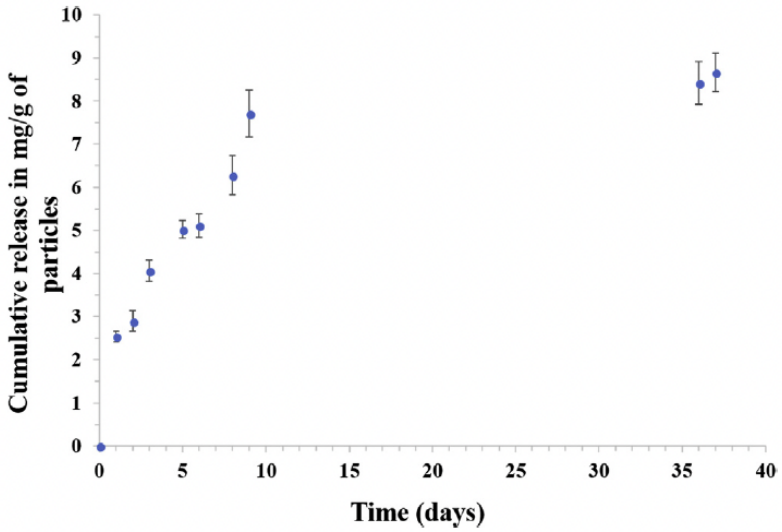

Fig. 5. Sulindac cumulative release profile from the particles synthesized by loading the reactor with 1 wt% sulindac.

Fig. 5 shows the cumulative release of sulindac and evidences a Burst effect after 24 h, followed by a quite linear release between 1 and 10 days that then levels until 37 days when a complete release is

Published in : International Journal of Pharmaceutics (2018), vol. 549, pp. 161–168
DOI: 10.1016/j.ijpharm.2018.07.060
Status : Postprint (Author's version)

reached. Between 10 days and 37 days, the sulindac release stops because the particles become empty. From the amount of released sulindac measured after 37 days (i.e. 8.6 mg), a particle loading corresponding to 8.6 mg per gram of particles can be calculated. Such loading corresponds to a drug encapsulation efficiency of 86% for the entire developed $scCO_2$ and photocleavage process. It is important to mention that the released sulindac possesses the same spectroscopic signature as the initial sulindac engaged in the encapsulation process as confirmed by UV–VIS spectrum. These results show that at least 86% of the initial sulindac remains unaltered by the whole encapsulation process that includes the polymerization in $scCO_2$ and the photocleavage in TFT. Since we have determined above that 2% of this sulindac is not encapsulated at the end of the $scCO_2$ polymerization, it means that only 12% of the initial sulindac is altered and/or lost during the encapsulation process.

Fig. 6 shows the daily release for the first 9 days. In the Burst effect observed in the first 24 h, 25% of the loaded sulindac is released. Then, a quite linear controlled release of about 500 µg/g per day is observed over the whole period of 8 days. After 9 days, 88% of the total load is thus released.

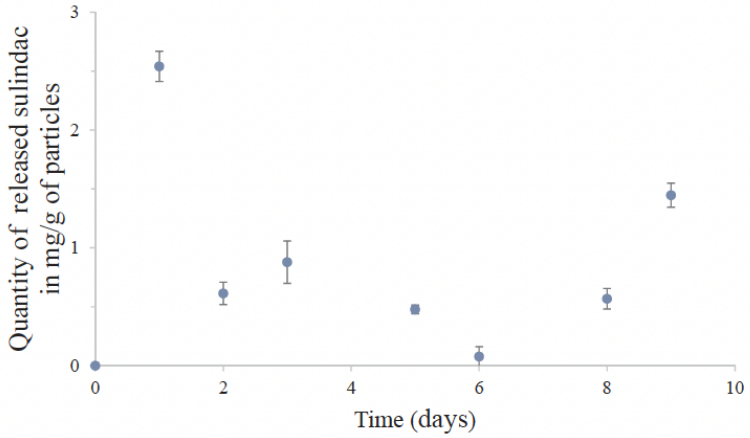

Fig. 6. Sulindac release profile per day from the particles loaded with 1 wt% sulindac.

As recently reported by Scavo et al., 2015, encapsulation of the NSAIDs such as sulindac in drug delivery systems is expected to increase the therapeutic effect along with decreasing the side effect for long-term administration. Our encapsulation process, allowing a constant release over 9 days might be quite promising especially for locoregional treatment, e.g. placing the particles during a surgery, to insure a sustained release of the sulindac during a few days. Due to this, we believe that encapsulation of a chemopreventive drug such as sulindac in a facile method is very interesting from the production and medical point of view.

3.3. GRAFTING ON THE PARTICLE SURFACES

As discussed above, selecting a stabiliser (PEO-*hv*-PFDA) that exhibit a photocleavable o-nitrobenzyl group at the junction of the blocks of the copolymer allows the removal at least partially of the fluorinated block modifying the release kinetics of sulindac. Looking closer to the photoreaction

Published in : International Journal of Pharmaceutics (2018), vol. 549, pp. 161–168
DOI: 10.1016/j.ijpharm.2018.07.060
Status : Postprint (Author's version)

(scheme 2), the light-induced cleavage of o-nitrobenzyl group generates a nitrosobenzaldehyde group at the end of the PEO segment entangled in the poly(HEMA) particles. These aldehyde groups located at the external periphery of the particles could be useful to further functionalisation of the particle surfaces. For instance, different probes for imaging or targeting could be grafted thanks to the aldehyde reactivity.

In the present study, the aldehyde groups have been used for grafting a fluorescent probe, i.e. the fluoresceinamine on the particle surface by using reductive amination. Reported conditions for reductive amination reaction by Freichels et al. (2012) have been followed as described in details in the experimental part. Extensive washing (i.e 3 days) by dialysis had been carefully performed after grafting. In order to eliminate the excess amount of fluoresceinamine that is not grafted onto the particles.

While before reaction with fluoresceinamine, the particles exhibit no fluorescence (not shown), they clearly emit the typical green light of the grafted fluorescein as it can be seen from the fluorescence microscope image (Fig. 7). This confirms that the developed process is able not only to provide particles allowing a sustained release of the encapsulated drug but also that the particles can be labelled with fluorescent probe by taking profit of the reactive groups generated by the photocleavage.

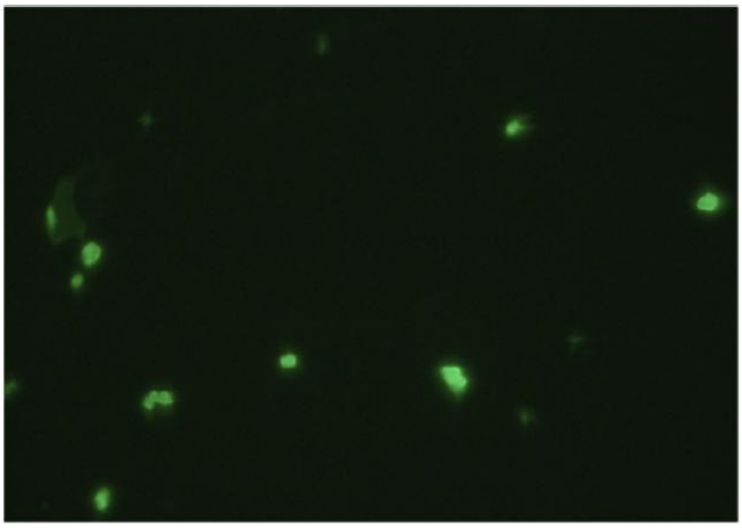

Fig. 7. The fluorescence microscopy images of the particles tagged with fluorescent probe.

4. Conclusions

One-pot encapsulation of sulindac in poly(HEMA) networks was successfully performed in supercritical carbon dioxide. The poly (HEMA) networks with or without sulindac were both produced with monodispersity and well-defined morphology and small size (271 nm). The $scCO_2$ can be removed

from the reaction medium by simple depressurisation which eliminates the reaction work-up step for purification and/or drying and leads after venting to the loaded particles as a dry powder with only 1.8% of remaining free sulindac for a targeted loading of 1%.

In addition, by using a photocleavable stabiliser, part of the fluorinated block can be extracted from the surface allowing the particles to be dispersed and swollen in aqueous media. Already after 30 min. of UV-photolysis, extensive swelling of the particles is observed when placed in water leading to swollen microgels of about 2.7 µm with an encapsulation efficiency of 86%.

Interestingly, after photocleavage, the generated aldehyde functions on the particle surface enables to perform further chemical functionalization with amine derivatives. As a proof of concept, a fluorescent dye was grafted by using fluoresceinamine leading to particles that can be detected by fluorescence microscope. This reductive amination step performed in aqueous media could be applied to a variety of amino-functional (macro)molecules of use for imaging or targeting. The described process allows thus to produce in few steps, well-defined multifunctional microgels. Thanks to mild reaction conditions (i.e 35 °C) and the non-toxic, inert and environmentally friendly polymerisation medium ($scCO_2$), this process could be extended to heat or solvent-sensitive API and constitutes a promising process for advanced formulations.

Acknowledgements

Authors thank the European financial support in the frame of the NanoFar program, an Erasmus Mundus Joint Doctorate (EMJD) program in nanomedicine and pharmaceutical innovation. CERM and BSMA are indebted to Interuniversity Attraction Poles (IAP-7/5-FS2). CERM thank the Region Wallonne DGO6 for funding research in the frame of the Smartdif project.

References

Abraham, S., Brahim, S., Ishihara, K., Guiseppi-Elie, A., 2005. Molecularly engineered p (HEMA)-based hydrogels for implant biochip biocompatibility. Biomaterials 26, 4767–4778. https://doi.org/10.1016/j.biomaterials.2005.01.031.

Alaimo, D., Grignard, B., Kuppan, C., Adriaensen, Y., Genet, M.J., Dupont-Gillain, C., Gohy, J.-F., Fustin, C.-A., Detrembleur, C., Jérôme, C., 2017. A photocleavable stabilizer for the preparation of PHEMA nanogels by dispersion polymerization in supercritical carbon dioxide. Polym. Chem. 8, 581–591. https://doi.org/10.1039/ C6PY01633B.

Ammar, H.O., El-Nahhas, S.A., Ghorab, M.M., Salama, A.H., 2012. Chitosan/cyclodextrin nanoparticles as drug delivery system. J. Incl. Phenom. Macrocycl. Chem. 72, 127–136. https://doi.org/10.1007/s10847-011-9950-5.

Andrade-vivero, P., Fernandez-gabriel, E., Alvarez-lorenzo, C., Concheiro, A., 2007. Improving the loading and release of NSAIDs from pHEMA hydrogels by copolymerization with functionalized monomers. J. Pharm. Sci. 96, 802–813. https://doi.org/10.1002/jps.

Published in : International Journal of Pharmaceutics (2018), vol. 549, pp. 161–168
DOI: 10.1016/j.ijpharm.2018.07.060
Status : Postprint (Author's version)

Badri, W., Miladi, K., Nazari, Q.A., Greige-Gerges, H., Fessi, H., Elaissari, A., 2016. Encapsulation of NSAIDs for inflammation management: overview, progress, challenges and prospects. Int. J. Pharm. 515, 757–773. https://doi.org/10.1016/j. ijpharm.2016.11.002.

Cadotte, A.J., Demarse, T.B., 2005. Poly-HEMA as a drug delivery device for in vitro neural networks on micro-electrode arrays. J. Neural Eng. 2, 114–122. https://doi. org/10.1088/17412560/2/4/007.

Cao, L., Chen, L., Chen, X., Zuo, L., Li, Z., 2006. Synthesis of smart core-shell polymer in supercritical carbon dioxide. Polymer (Guildf) 47, 4588–4595. https://doi.org/10.1016/j.polymer.2006.04.039.

Carmona-Moran, C.A., Zavgorodnya, O., Penman, A.D., Kharlampieva, E., Bridges, S.L., Hergenrother, R.W., Singh, J.A., Wick, T.M., 2016. Development of gellan gum containing formulations for transdermal drug delivery: component evaluation and controlled drug release using temperature responsive nanogels. Int. J. Pharm. 509, 465–476. https://doi.org/10.1016/j.ijpharm.2016.05.062.

Chacko, R.T., Ventura, J., Zhuang, J., Thayumanavan, S., 2012. Polymer nanogels: a versatile nanoscopic drug delivery platform. Adv. Drug Deliv. Rev. 64, 836–851. https://doi.org/10.1016/j.addr.2012.02.002.

Choudhary, S., Reck, J.M., Carr, A.J., Bhatia, S.R., 2017. Hydrophobically modified alginate for extended release of pharmaceuticals. Polym. Adv. Technol. 1–7. https:// doi.org/10.1002/pat.4103.

Cocero, M.J., Martín, Á., Mattea, F., Varona, S., 2009. Encapsulation and co-precipitation processes with supercritical fluids: fundamentals and applications. J. Supercrit. Fluids. https://doi.org/10.1016/j.supflu.2008.08.015.

Davies, O.R., Lewis, A.L., Whitaker, M.J., Tai, H., Shakesheff, K.M., Howdle, S.M., 2008. Applications of supercritical CO2 in the fabrication of polymer systems for drug delivery and tissue engineering. Adv. Drug Deliv. Rev. 60, 373–387. https://doi.org/10.1016/j.addr.2006.12.001.

Freichels, H., Alaimo, D., Auzély-Velty, R., Jérôme, C., 2012. α-Acetal, ω-Alkyne Poly (ethylene oxide) as a versatile building block for the synthesis of glycoconjugated graft-copolymers suited for targeted drug delivery. Bioconjug. Chem. 23, 1740–1752. https://doi.org/10.1021/bc200650n.

Garcia-Millan, E., Koprivnik, S., Otero-Espinar, F.J., 2015. Drug loading optimization and extended drug delivery of corticoids from pHEMA based soft contact lenses hydrogels via chemical and microstructural modifications. Int. J. Pharm. 487, 260–269. https:// doi.org/10.1016/j.ijpharm.2015.04.037.

Gerstein, N.S., Gerstein, W.H., Carey, M.C., Lam, N.C.K., Ram, H., Spassil, N.R., Schulman, P.M., 2014. The thrombotic and arrhythmogenic risks of perioperative NSAIDs. J. Cardiothorac. Vasc. Anesth. 28, 369–378. https://doi.org/10.1053/j.jvca. 2013.05.018.

González-Chomón, C., Braga, M.E.M., De Sousa, H.C., Concheiro, A., Alvarez-Lorenzo, C., 2012. Antifouling foldable acrylic IOLs loaded with norfloxacin by aqueous soaking and by supercritical carbon dioxide technology. Eur. J. Pharm. Biopharm. 82, 383–391. https://doi.org/10.1016/j.ejpb.2012.07.007.

Guerra, R.B., Gálico, D.A., Holanda, B.B.C., Bannach, G., 2016. Solid-state thermal and spectroscopic studies of the anti-inflammatory drug sulindac using UV-Vis, MIR, NIR, DSC, simultaneous TG-DSC, and the coupled techniques TG-EGA-MIR and DSC-optical microscopy. J. Therm. Anal. Calorim. 123, 2523–2530. https://doi.org/10.1007/s10973-015-5228-2.

Hackl, E.V., Khutoryanskiy, V.V., Ermolina, I., 2017. Hydrogels based on copolymers of 2hydroxyethylmethacrylate and 2-hydroxyethylacrylate as a delivery system for proteins: interactions with lysozyme. J. Appl. Polym. Sci. 134, 1–13. https://doi.org/10. 1002/app.44768.

Hamidi, M., Azadi, A., Rafiei, P., 2008. Hydrogel nanoparticles in drug delivery. Adv. Drug Deliv. Rev. 60, 1638–1649. https://doi.org/10.1016/j.addr.2008.08.002.

Jennings, J., Beija, M., Kennon, J.T., Willcock, H., Reilly, R.K.O., Rimmer, S., Howdle, S.M., 2013. Advantages of block copolymer synthesis by RAFT-controlled dispersion polymerization in supercritical carbon dioxide. Macromolecules 46, 6843–6851.

Kitagawa, H., Takeda, K., Kitagawa, R., Izutani, N., Miki, S., Hirose, N., Hayashi, M., Imazato, S., 2014. Development of sustained antimicrobial-release systems using poly (2-hydroxyethyl methacrylate)/trimethylolpropane trimethacrylate hydrogels. Acta Biomater. 10, 4285–4295. https://doi.org/10.1016/j.actbio.2014.06.016.

Lee, J.K., Paine, M.F., Brouwer, K.L.R., 2010. Sulindac and its metabolites inhibit multiple transport proteins in rat and human hepatocytes. J. Pharmacol. Exp. Ther. 334, 410–418. https://doi.org/10.1124/jpet.110.165852.

Long, T.J., Sprenger, C.C., Plymate, S.R., Ratner, B.D., 2014. Prostate cancer xenografts engineered from 3D precision-porous poly(2-hydroxyethyl methacrylate) hydrogels as models for tumorigenesis and dormancy escape. Biomaterials 35, 8164–8174. https://doi.org/10.1016/j.biomaterials.2014.04.090.

Ma, Z., Lacroix-desmazes, P., 2004. Dispersion polymerization of 2-hydroxyethyl methacrylate stabilized by a hydrophilic/CO2-philic poly (ethylene diblock copolymer in supercritical carbon dioxide. Polym. J. 45, 6789–6797. https://doi.org/10.1016/j. polymer.2004.07.065.

Macková, H., Plichta, Z., Hlídková, H., Sedláček, O., Konefal, R., Sadakbayeva, Z., Dušková-Smrčková, M., Horák, D., Kubinová, Š., 2017. Reductively degradable poly (2-hydroxyethyl methacrylate) hydrogels with oriented porosity for tissue engineering applications. ACS Appl. Mater. Interfaces 9, 10544–10553. https://doi.org/ 10.1021/acsami.7b01513.

Miyazaki, Y., Aruga, N., Kadota, K., Tozuka, Y., Takeuchi, H., 2017. Improved respirable fraction of budesonide powder for dry powder inhaler formulations produced by advanced supercritical CO2 processing and use of a novel additive. Int. J. Pharm. 528, 118–126. https://doi.org/10.1016/j.ijpharm.2017.06.002.

Nuchuchua, O., Nejadnik, M.R., Goulooze, S.C., Lješković, N.J., Every, H.A., Jiskoot, W., 2017. Characterization of drug delivery particles produced by supercritical carbon dioxide technologies. J. Supercrit. Fluids 128, 244–262. https://doi.org/10.1016/j. supflu.2017.06.002.

Parilti, R., Alaimo, D., Grignard, B., Boury, F., Howdle, S.M., Jérôme, C., 2017. Mild synthesis of poly(HEMA)-networks as well-defined nanoparticles in supercritical carbon dioxide. J. Mater. Chem. B 5, 5806–5815. https://doi.org/10.1039/ C7TB00740J.

Ryu, J.-H., Chacko, R.T., Jiwpanich, S., Bickerton, S., Babu, R.P., Thayumanavan, S., 2010. Self-cross-linked polymer nanogels: a versatile nanoscopic drug delivery platform. J. Am. Chem. Soc. 132, 17227–17235. https://doi.org/10.1021/ja1069932.

Singh, R., Cadeddu, R.-P., Fröbel, J., Wilk, C.M., Bruns, I., Zerbini, L.F., Prenzel, T., Hartwig, S., Brünnert, D., Schroeder, T., Lehr, S., Haas, R., Czibere, A., 2011. The non-steroidal anti-

inflammatory drugs Sulindac sulfide and Diclofenac induce apoptosis and differentiation in human acute myeloid leukemia cells through an AP-1 dependent pathway. Apoptosis 16, 889–901. https://doi.org/10.1007/s10495-0110624-y.

Scavo, M.P., Gentile, E., Wolfram, J., Gu, J., Barone, M., Evangelopoulos, M., Martinez, J.O., Liu, X., Celia, C., Tasciotti, E., Vilar, E., Shen, H., 2015. Multistage vector delivery of sulindac and silymarin for prevention of colon cancer. Colloids Surface B Biointerfaces 136, 694–703.